catalysts

MDPI

Article

Simulation of Denitrification of Vehicle Exhaust over Cu-CHA Bazite Catalyst for a Monolith Reactor

Yanxia Li *, Yuwen Zhu, Ning Zhang and Zhongliang Liu

MOE Key Laboratory of Enhanced Heat Transfer and Energy Conservation, Beijing Key Laboratory of Heat Transfer and Energy Conversion, College of Environmental and Energy Engineering, University of Technology, Ping Le Yuan 100, Beijing 100124, China; zhuyw@emails.bjut.edu.cn (Y.Z.); ZhangN@emails.bjut.edu.cn (N.Z.); liuzhl@bjut.edu.cn (Z.L.)

* Correspondence: liyanxia@bjut.edu.cn; Tel.: +86-13671359425

Abstract: A CFD model with chemical reaction kinetic and heat and mass transfer for a monolith reactor is established by COMSOL Multiphysics to investigate the influence of different operating conditions and water on denitrification efficiency for Cu-CHA. At the low temperature range, water has little effect on the denitrification efficiency over the Cu-CHA catalyst while NO conversion is increased by about 30% at the medium temperature. The concentration of O_2 (C_{O2}) has no significant effect on the performance of Cu-CHA catalyst. The best ratio of NO_2 to NO_x in feed gases may be 1/2, which improves the denitrification efficiency and the yield of N_2 but it produces relatively little N_2O. The optimal ammonia-nitrogen ratio is 1.1, where Cu-CHA catalyst has fairly great denitrification efficiency and low NH_3 leakage. Increasing inlet flow velocity and cross area of channels have negative effect on NO conversion, while longer channels and thicker substrate have the opposite effect.

Keywords: denitrification; Cu-CHA; SCR; water resistant; numerical study

check for updates

Citation: Li, Y.; Zhu, Y.; Zhang, N.; Liu, Z. Simulation of Denitrification of Vehicle Exhaust over Cu-CHA Bazite Catalyst for a Monolith Reactor. *Catalysts* **2021**, *11*, 930. https://doi.org/10.3390/catal11080930

Academic Editor: Antonella Gervasini

Received: 26 June 2021
Accepted: 28 July 2021
Published: 30 July 2021

Publisher's Note: MDPI stays neutral with regard to jurisdictional claims in published maps and institutional affiliations.

Copyright: © 2021 by the authors. Licensee MDPI, Basel, Switzerland. This article is an open access article distributed under the terms and conditions of the Creative Commons Attribution (CC BY) license (https://creativecommons.org/licenses/by/4.0/).

1. Introduction

Due to the high energy consumption, the environmental pollution caused by the use of non-renewable energy needs to be solved urgently. Diesel vehicle exhaust contains a large amount of nitrogen oxide, which poses threats to human health and the environment. As one of the most mature and widest used technology for denitrification, selective catalytic reduction with ammonia (NH_3-SCR) has been studied in various aspects. According to the different reaction rate, NH_3-SCR can be divided into three types: standard SCR (Equation (1)), fast SCR (Equation (2)) and NO_2-SCR (Equation (3)):

$$4NH_3 + 4NO + O_2 \rightarrow 4N_2 + 6H_2O \quad (1)$$

$$2NH_3 + NO + NO_2 \rightarrow 2N_2 + 3H_2O \quad (2)$$

$$8NH_3 + 6NO_2 \rightarrow 7N_2 + 12H_2O \quad (3)$$

The reason why the fast SCR has a faster reaction rate than the standard SCR is that the oxidation ability of NO_2 is stronger than that of O_2. However, the share of NO_2 in diesel exhaust is about 5%, so NO_2-SCR becomes known as slow SCR. Therefore, the ratio of NO_2 in the feed gases is very important. Also, some researches on the influence of NO_2 on Cu-SSZ-13 [1], Cu-SSZ-39 [2], Cu-T3 [3] etc. indicate that NO_2 can result in the promotion of NO_x conversion.

Many kinds of catalysts have been found to be used in NH_3-SCR because of the active sites on their surface that can adsorb NO_x in vehicle exhaust. As so far, catalysts applied to NH_3-SCR are generally used at medium and high temperature, and have poor water and sulfur resistance, such as commercial V_2O_5-TiO_2. Hence, it is necessary

to explore replaceable catalysts. Generally speaking, Cu-zeolite catalyst has better low-temperature performance and higher NH_3-storage capacity [4]. Although a large number of experimental studies aimed to Cu-zeolite catalysts, most of them focused on cations doping, selection of molecular sieve carriers or the comparison of topological structures [5–7]. As to the simulation researches, the kinetic models for NH_3-SCR over vanadium-based catalysts only involved standard SCR and ammonia oxidation [8,9]. To zeolite catalyst, however, most researches were concerned about powdered catalysts or reaction in single channel model [10–12], which is not in line with the actual situation. Only a few of researches investigated the NH_3-SCR in a monolithic reactor using Cu-zeolite as catalysts [13,14].

Among the zeolites, the chabazite (CHA) has a large surface area and high porosity as a result of microporous topological structure, which makes them one of the most popular NH_3-SCR candidates for the catalyst carrier. Thus, Cu-CHA catalysts are more attractive. Many experimental studies have proved that water has a positive influence on the denitrification efficiency of Cu-CHA [15–17] and drawn a common conclusion that Cu-CHA has an excellent hydrothermal stability. Contrary to other metals or their oxide catalysts, water can increase the NO conversion on Cu-CHA, which makes Cu-CHA a quite suitable catalyst for NH_3-SCR. However, few studies have been done on water effect, especially in simulation studies using a global kinetic mechanism. Fahami, et al. [18] explored the effects of gas hourly space velocity (GHSV), NO, O_2, NO_2 and H_2O concentration on NO conversion with a detailed kinetic mechanism for NO oxidation on Cu-CHA at low and medium temperature (150–350 °C). In their studies, the experimental data and simulation results fit well and the parameters of the mathematical model in each chemical reaction step were illustrated. They also found that increasing GHSV and the concentration of H_2O and NO_2 could inhibit NO oxidation, while O_2 could promote it. Active sites may perform diversely at different reaction temperatures. Olsson, et al. [11] established a multi-sites kinetic model containing NH_3 storage, release and oxidation, standard SCR and N_2O formation in 100–600 °C with 5% H_2O in feed gases, but fast SCR and NO_2 SCR were not included. The results showed that different NH_3 adsorption temperatures corresponded to different sites. They also suggested that standard SCR mainly took place on site 1 and NH_3 oxidation was major on site 2. Besides, Gao, et al. [19] built a comprehensive model with two adsorption sites and global kinetic reactions, which was a rare model including low temperature H_2O storage on site 2.

In summary, most of the research focused on catalysts themselves. However, the structural design of a NH_3-SCR monolith catalyst reactor is lack of the theoretical support. Thus, a global kinetic mechanism is used to simulate the chemical reactions of NO_x over Cu-based monolith catalyst and study the influence of different operating conditions, such as inlet velocity of reactants, the length of channels etc., providing reference for engineering design and evaluating the performance of Cu-CHA monolith catalyst. When the reactant gases flow through the porous monolith catalyst, the selective catalytic reactions occur on the support surface accompanied by heat and mass transfer. Hence, a mathematical model for predicting heterogeneous reactions, flow, mass and heat transfer characteristics of $NO_x/NH_3/H_2O/N_2$ mixture flowing in a honeycomb cordierite ceramic monolith with Cu-CHA washcoating is established by commercial software COMSOL Multiphysics. And the chemical kinetic model includes ammonia oxidation, nitrogen oxidation, standard, fast and slow SCR reactions, NH_4NO_3 and N_2O formation and decomposition. Also the presence of H_2O in feed gases impacts on the denitrification efficiency of Cu-CHA is studied.

2. Results and Discussion

2.1. Effect of the Presence of H_2O in Reactant Mixture

Figures 1 and 2 compare the NO and NH_3 conversion between simulated and experimental values under various operating conditions. As can be seen from Figures 1 and 2, it reveals that water evidently improves the ability of Cu-CHA to convert NO at medium temperature, with an increase of 30.468% (experiment) and 27.947% (simulation). And

it increases NH_3 conversion by 10.341% (experiment) and 29.597% (simulation) at low temperature. Under both operating conditions, NO conversion climbs at low temperature, peaks to maximum at 250 °C, then decline at medium temperature. And Figure 2 shows rapidly rise of NH_3 conversion, followed by a muted growth after 250 °C, and then it reaches approximate 100% eventually. H_2O also decreases the temperature for Cu-CHA reaching maximum NH_3 conversion. The finding is different from the well-known result that H_2O would inhibit the NH_3-SCR reactions over other metals and their oxide catalysts, due to the active sites competition among H_2O and reactants (NH_3 and NO) or forming nitrate accumulating on the surface of the catalysts [20–22]. The special feature of Cu-CHA makes it a very suitable catalyst for NH_3-SCR, because H_2O is abundant in diesel vehicle exhaust and it is produced by NH_3-SCR reaction as well. Actually, this phenomenon is probably due to H_2O inhibits ammonia oxidation, which occurs at the temperature higher than 300 °C. And at low temperature, this effect may attribute to the enhancement of Cu reducibility and the increase of Bronsted acidity, resulting in more NH_3 to be absorbed [16]. The enhancement of NH_3 conversion means a reduction of the possibility of NH_3 leakage.

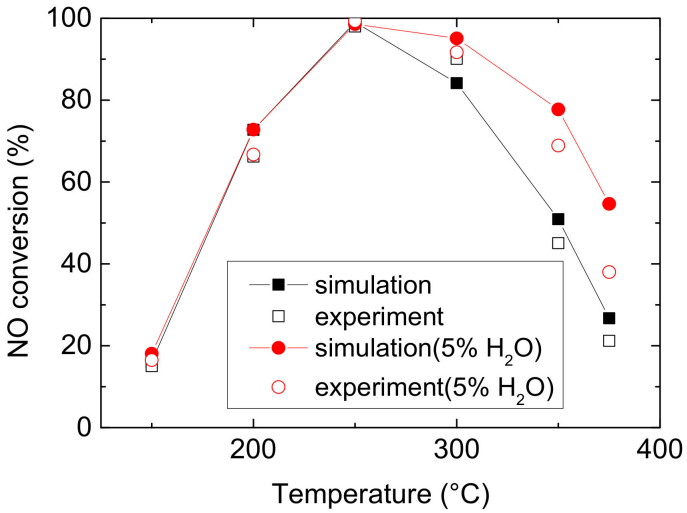

Figure 1. NO conversion comparison of experimental and simulated values in 150–375 °C [23].

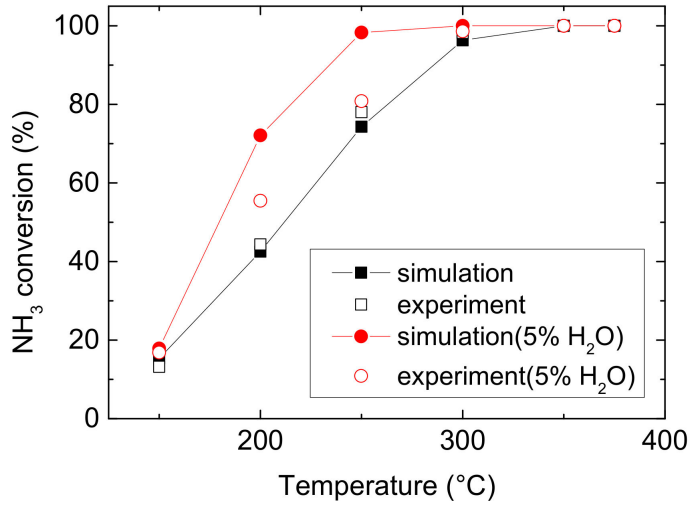

Figure 2. NH_3 conversion comparison of experimental and simulated results in 150–375 °C [23].

2.2. Effects of Reactant Gas Composition

2.2.1. Effect of Concentration of O_2

Oxygen participates in most reactions in the global kinetic model of NH_3-SCR, for instance, NH_3 oxidation, NO oxidation, N_2O decomposition. And it plays an important role in determining the dominant reaction among standard SCR, fast SCR and NO_2-SCR. So, it is necessary to study the effect of C_{O2} on denitrification efficiency. Figure 3 shows the simulated results of NO conversion with 0.1%, 2% and 6% O_2 in feed gas. From Figure 3, it can be seen that with the increase of C_{O2}, NO conversion has little improvement. The more O_2 could stimulate standard SCR (Equation (1)) and promote NO oxidizing to more NO_2, which is help to fast SCR (Equation (2)). However, because NO and NO_2 have higher oxidation ability than O_2 and the concentration of reactants is low in this model, the difference is not obvious.

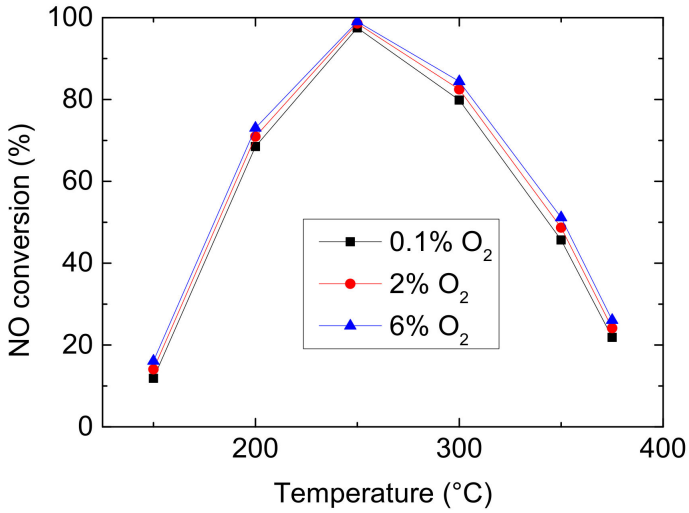

Figure 3. Effect of C_{O2} on NO conversion (Reaction temperature T = 150–375 °C, Concentration $C_{NH3} = C_{NO}$ = 750 ppm, without H_2O).

2.2.2. Effect of Concentration of NO_2

In fact, NO accounts for 90–95% of NO_x in diesel exhaust due to a high burning temperature inside the internal combustion engine. NO would be partially converted into NO_2, the reaction equation is given by:

$$2NO + O_2 \leftrightarrow 2NO_2 \quad (4)$$

This equilibrium is reversible, and Shin, et al. [24] believe that the reaction is thermodynamically controlled above 270 °C and kinetically controlled below 270 °C. The percentage of NO_2 in reactant gases plays an important role in reduction of NO_x. Defining x_0 as the ratio of NO_2 to NO_x, x_0 varies from 0 to 1. $x_0 = \frac{C_{NO_2}}{C_{NO_x}} = \frac{C_{NO_2}}{C_{NO}+C_{NO_2}}$. Here, C_i is the concentration of reactant i.

In this study, five operating conditions were selected to simulate outlet concentration of NO, N_2 and N_2O. As shown in Table 1, it includes inlet concentrations of components corresponding to different x_0. Figures 4 and 5 illustrate the outlet concentrations of NO and N_2, as a function of the reaction temperature and x_0 respectively.

Table 1. x_0 and the corresponding inlet concentrations of components used for simulation.

x_0	C_{NH3} (ppm)	C_{NO} (ppm)	C_{NO2} (ppm)	C_{O2} (%)	C_{H2O} (%)
0	750	750	0	6	5
0.25	750	562.5	187.5	6	5
0.5	750	375	375	6	5
0.75	750	187.5	562.5	6	5
1	750	0	750	6	5

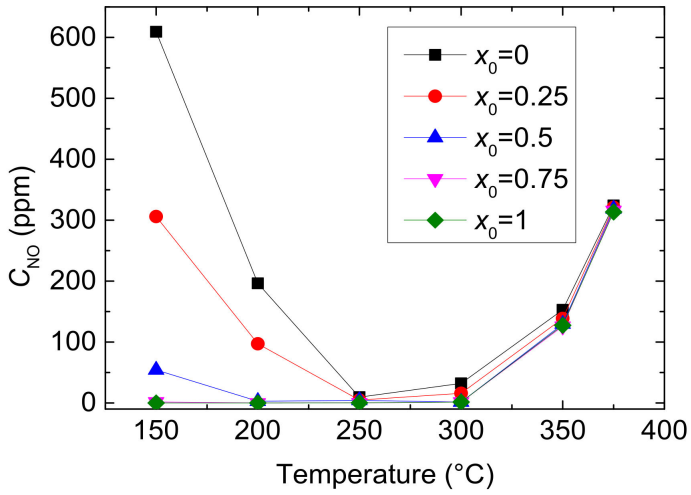

Figure 4. Outlet C_{NO} with different values of x_0 and reaction temperatures.

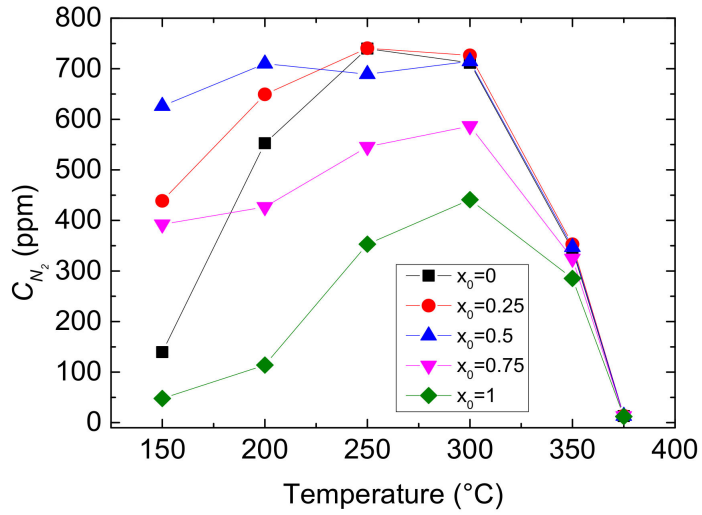

Figure 5. Outlet C_{N2} with different values of x_0 and reaction temperatures.

As shown in Figure 4, the outlet C_{NO} reduces to a minimum at 250 °C and then gradually rises under each x_0. And at the same reaction temperature, with the increase of value of x_0, the outlet C_{NO} significantly decreases, indicating the presence of NO_2 in feed gas has a positive influence on NO conversion. When x_0 is larger than 0.5, the outlet C_{NO} is close to zero within the range of 200–300 °C, which means that the inlet NO has almost been converted to NO_2 or N_2. As can be seen from Figure 5, reaction temperature and the value of x_0 greatly influences the yield of N_2. The outlet C_{N2} peaks to maximum at 250 °C when $x_0 \leq 0.25$ and at 300 °C when $x_0 \geq 0.25$, then it decline sharply. Furthermore, as the value of x_0 growing, the yield of N_2 increases and then decreases under the same temperature. Actually, different values of x_0 mean different C_{NO2} in feed gases

and can result in a different selective catalytic reaction. Generally speaking, x_0 = 0–0.5 is the transition period from standard SCR to fast SCR and x_0 = 0.5–0.75 is fast SCR to NO_2-SCR. The result demonstrates that standard SCR prevails most at 250 °C while fast SCR at 300 °C. Due to the oxidation ability of NO_2 being better than that of O_2, NO_2 reacts more easily with NH_3 than O_2 at low temperature. Therefore, larger C_{NO2} can contribute to a higher NO conversion by fast SCR. But, overmuch x_0 make NO_2-SCR gradually prevail which need more NH_3 to react, and it slows down the fast SCR reaction, resulting in a decrease in yield of N_2.

Although increasing the value of x_0 can improve NH_3-SCR, the C_{N2O} in outlet mixture might increase if NO_2-SCR dominants. N_2O is formed from ammonium nitrate by thermal decomposition through NO_2-SCR at low temperature:

$$NH_3 + 2NO_2 \leftrightarrow NH_4NO_3 + N_2 + H_2O \quad (5)$$

$$NH_4NO_3 \rightarrow N_2O + 2H_2O \quad (6)$$

These two chemical reactions have negative impacts on NO_x conversion. On the one hand, the nitrification may cover active sites and cause the devaluation of catalyst activity. On the other hand, N_2O is one of greenhouse gases and its GWP (global warming potential) is about 298 times than that of CO_2. Figure 6 shows the outlet C_{N2O} as a function of the reaction temperature and the value of x_0.

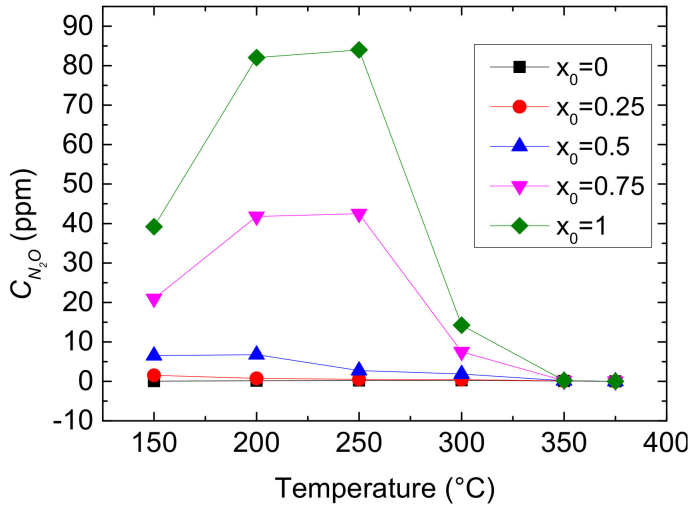

Figure 6. Outlet C_{N2O} as different x_0 values and reaction temperatures.

As shown in Figure 6, the rise of x_0 causes an overall increase of outlet C_{N2O}, especially in 150–300 °C. It also shows that the outlet C_{N2O} firstly increases and then decreases with the growth of reaction temperature when $x_0 > 0.5$, however, the concentration slowly falls when $x_0 \leq 0.5$. It indicates that N_2O production being from the decomposition of ammonium nitrate happens at low temperature for Cu-CHA when NO_2 is more, and higher temperature inhibits it.

Based on Figures 4–6, it comes to the conclusion that the balanced point is x_0 = 0.5. Under this operating condition, Cu-CHA catalyst has a high yield of N_2 and quite low outlet concentrations of NO and N_2O, giving a large NO conversion and better performance.

2.2.3. Effect of Ammonia to NO_x Ratio (ANR)

ANR is regarded as the ratio of NH_3 to NO_x and can be defined as the following formula: $\text{ANR} = \frac{C_{NH_3}}{C_{NO_x}}$. According to Equations (1)–(3), standard SCR and fast SCR prevail as ANR = 1. When ANR > 1.0, NH_3 is overmuch and NO_2-SCR prevails, resulting in weak catalytic ability. However, to ensure high denitrification efficiencies, excessive

NH_3 is supplied to SCR equipment to prohibit NH_3 oxidation and inadequate reaction, etc., which has a risk of NH_3 leakage and environment pollution. Thus, four operating conditions are designed to investigate the best ANR value. Table 2 lists four ANR values and corresponding inlet concentrations of mixture gases used for simulation. And Figures 7 and 8 show the outlet concentrations of NO and NH_3 with different values of ANR and reaction temperatures.

Table 2. ANR and the corresponding inlet concentrations of NH_3, NO, O_2 and H_2O.

ANR	C_{NH3} (ppm)	C_{NO} (ppm)	C_{O2} (%)	C_{H2O} (%)
0.8	750	937.5	6	5
1	750	750	6	5
1.2	750	625	6	5
1.5	750	500	6	5

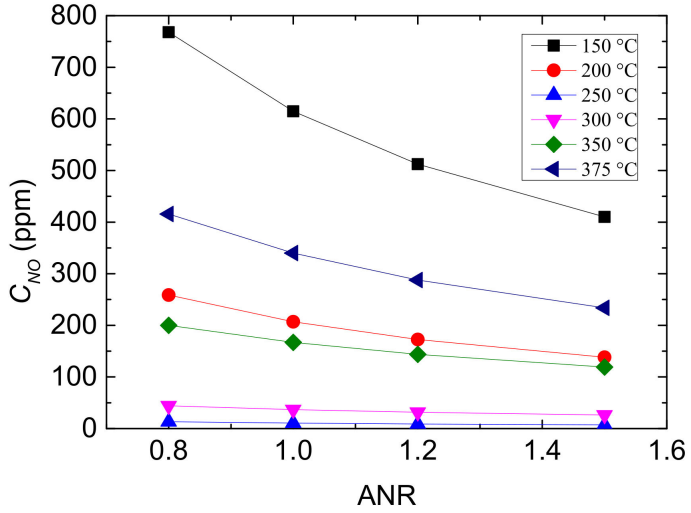

Figure 7. Outlet C_{NO} with different values of ANR and reaction temperatures.

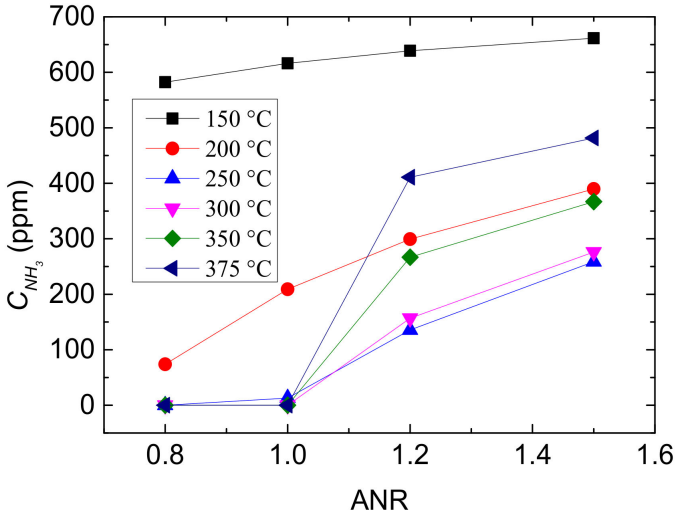

Figure 8. Outlet C_{NH3} with different values of ANR and reaction temperatures.

It can be seen from Figure 7 that the outlet C_{NO} all declines with the increase of ANR and it falls more obviously at the low and high temperature range, which indicates that the performance of Cu-CHA catalyst is improved with the increasing value of ANR. But the

decreasing trend of C_{NO} with ANR rising becomes flat, demonstrating that the influence of NH_3 increase is gradually limited. Especially when ANR $\geq$ 1.1, the decreasing rate is not greater than 20%, and the temperature influence it more rather than ANR. In addition, at 250 °C and 300 °C, outlet C_{NO} is lowest regardless of ANR value, owing to that reaction temperature is the other major factor to performance of Cu-CHA.

Subsequently, the relationship between ANR and outlet C_{NH3} at different reaction temperatures is displayed in Figure 8. The change trend of the C_{NH3} at 150 °C and 200 °C are different from that at the other temperature, which is higher than that at 250–375 °C when ANR $\leq$ 1.0. This is due to that oxidation of NH_3 and standard SCR mainly occurred at the medium to high temperature range. Besides, the C_{NH3} is near zero between ANR is 0.8–1.0 when T > 250 °C and it follows by sharply rise as ANR increasing. Therefore, supplying overmuch NH_3 would lead to leakage and is uneconomical.

Combining Figure 7 with Figure 8, it can be concluded that ANR approximately close to 1 is appropriate for Cu-CHA catalyst in NH_3-SCR. But, considering uncertainties of running status of vehicles, ANR = 1.1 would be more optimal. Under this operating condition, Cu-CHA performs relative lower outlet concentrations of NO and NH_3, showing higher NO conversion rate and less NH_3 leakage or waste.

2.3. Effect of Inlet Velocity

Currently, the common exhaust after-treatment equipment includes DOC (Diesel Oxidation Catalyst), DPF (Diesel Particulate Filter) and SCR. The monolith catalytic reactor used for NH_3-SCR is usually installed downstream of the exhaust treatment system. Thus, the speed of mixture entering into NH_3-SCR system has been much retarded. In this study, Reynolds number of mainstream flowing in the channels is 34.8, which can be treated as laminar flow. The change of NO conversion with various inlet flow velocity is shown in Figure 9.

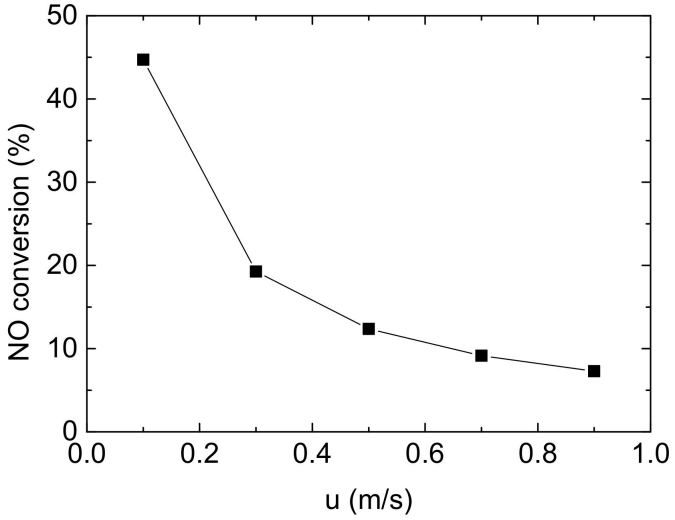

Figure 9. Effect of inlet flow velocity on NO conversion (Reaction temperature T = 150 °C, Concentration C_{NH3} = C_{NO} = 750 ppm, C_{O2} = 6%, without H_2O).

Five inlet flow velocities were studied in this study, from 0.1 m/s to 0.9 m/s, gradually increasing by 0.2 m/s. As the inlet velocity increasing, NO conversion decreases significantly from 44.717% to 19.255% from 0.1 m/s to 0.3 m/s, with a reduction of 56.94%. Subsequently, the trend become flatter after 0.3 m/s, indicating that the effect of inlet velocity on the denitrification of Cu-CHA gradually decrease. Due to the length of model is only 20 mm, the negative influence of increasing velocity on NO conversion is limited. Obviously, when other conditions remain unchanged, it can be considered that the contact time between the reactant gases and the catalyst is relatively short as velocity rising, resulting in insufficient reaction and deterioration of denitrification.

2.4. Effects of Structural Parameters

2.4.1. Length of Channels

The internal space of diesel vehicles limits the size of after-treatment equipment and leads to a restriction on the channel length of the monolith catalytic reactor, which will effect on NO conversion, as shown in Figure 10. This section aims to investigate the influence of the length of channels on NO conversion with control variates method.

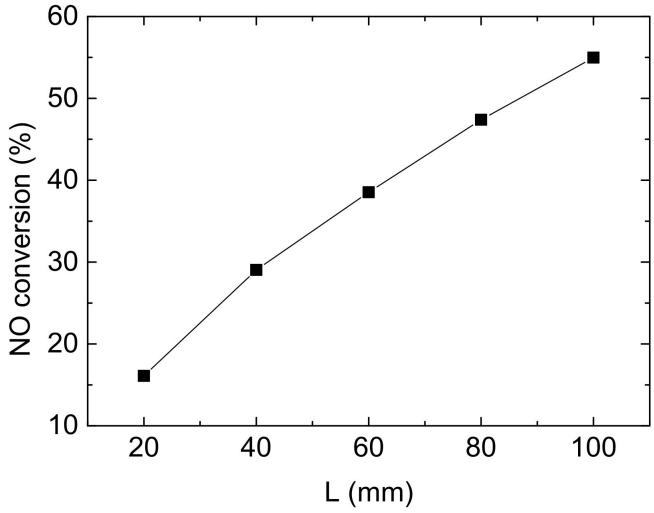

Figure 10. Influence of reactor length on NO conversion (Reaction temperature T = 150 °C, Concentration C_{NH3} = C_{NO} = 750 ppm, C_{O2} = 6%, without H_2O).

It can be clearly seen from the Figure 10 that NO conversion rises linearly with the increase of the length. When the length is increased by 20 mm, the denitrification efficiency is enhanced by about 10%. The longer channels provide more contact areas to reactant gases and the catalytic substrate. So, it could be predicted that NO conversion could reach a quite high value following this trend, probably 100%. However, it is unrealistic because the space of diesel vehicle and cost of reactor limit it. Hence, it needs more consideration in the practical application.

2.4.2. Cross Area of Channels

Besides, the cross areas of channels also affects NO conversion. Assuming other operating conditions remain constant, Figure 11 described the relationship between NO conversion and the cross area of channels.

In this part, only the side length of square channels varies, from 0.5 mm, 1 mm, 2 mm to 4 mm. And corresponding cross areas of square channels 'A' are 0.25 mm^2, 1 mm^2, 4 mm^2 and 16 mm^2 respectively. According to that, the area-volume ratios of single channel are 8, 4, 2 and 1. As shown in Figure 11, from 0.25 mm^2 to 1 mm^2, NO conversion decreases by 51.849%. After that, the reduction of the denitrification efficiency trends to be flat with the increase of cross area of channels, which means that the influence of cross areas is weaken. From the result described above, larger cross area (amount to smaller surface area) leads to smaller area-volume ratio at the same inlet velocity. The small contact area for reactant and catalyst surface results to the decline of NO conversion. Besides, by $Q_m = Av\rho$ (here Q_m is inlet mass flow rate), the larger A is equal to the higher Q_m. WHSV (weight hourly space velocity) is a ration to measure the reactant mass that can be treated by unit mass of catalyst in unit time, which is defined as: WHSV = inlet mass of exhaust gases/mass of Cu-CHA catalyst. Higher Q_m leads to larger WHSV, which also shrinks the reaction time and reduces denitrification efficiency.

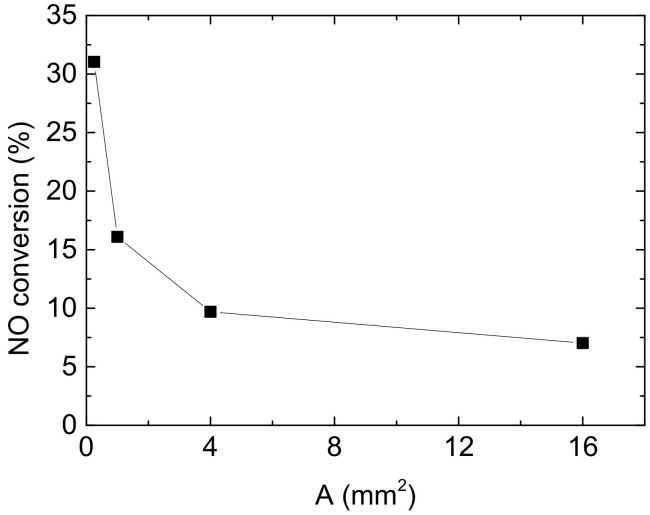

Figure 11. Influence of the cross area of channels on NO conversion (Reaction temperature T = 150 °C, Concentration C_{NH3} = C_{NO} = 750 ppm, C_{O2} = 6%, without H_2O).

2.4.3. Wall Thickness of Channels

In general, the monolithic catalysts are prepared by loading the active components on the walls of substrate. The reactants diffuse to surface of Cu-CHA catalyst and a part of them are adsorbed on the active sites. Figure 12 shows the influence of wall thickness of channels on NO conversion with control variates method.

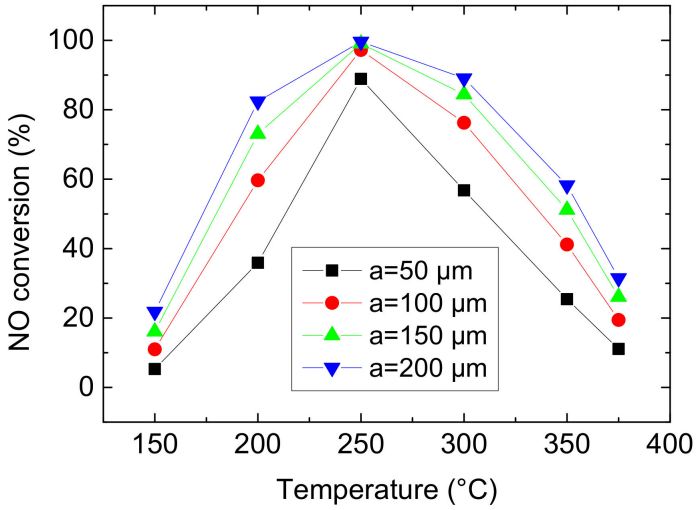

Figure 12. Effect of wall thickness of channels on NO conversion (Concentration C_{NH3} = C_{NO} = 750 ppm, C_{O2} = 6%, without H_2O).

In this section, the wall thickness of channels 'a' is set as 50 μm, 100 μm, 150 μm and 200 μm. As can be seen from the Figure 12, it has the maximum average growth rate of NO conversion from 50 to 100 μm. And then, the increasing trend slows down, especially when a varies from 150 to 200 μm, indicating that the influence of wall thickness is limited. On the one hand, from three-dimensional model in Figure 13, the thicker the substrate, the less number of channels and the more mass of Cu-CHA catalyst in per unit area (as setting the total mass of Cu-CHA is constant). On the other hand, due to fixed v and A, Q_m of mixture gases is also maintained. So, based on the above two points, the thicker wall leads to more contact between reactants and Cu-CHA catalyst but lower WHSV. In other words, lower WHSV signifies longer residence time of mixture gases which results in more complete

NH_3-SCR reaction and higher NO conversion. However, the effect of WHSV is finite when a varies from 150 to 200 μm, which may because the total mass of Cu-CHA catalyst is fixed.

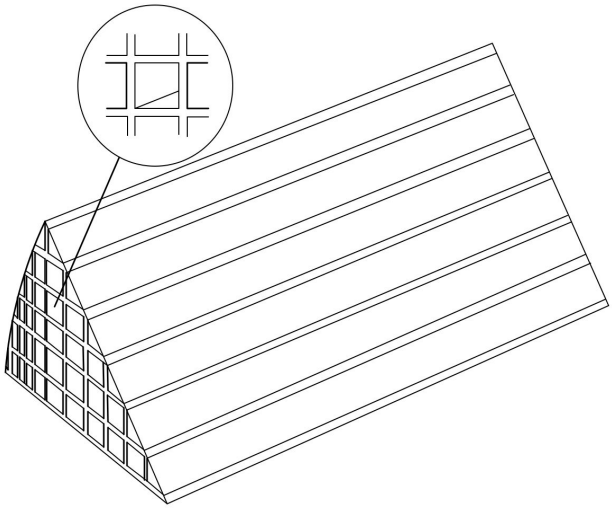

Figure 13. Cu-CHA monolithic catalytic reactor.

3. Simulation Methods

The geometric model of honeycomb monolith is established, as shown in Figure 13. In order to reduce running memory and save simulation time, only 1/8 of the reactor is used as the computational domain. And structural physical parameters of Cu-CHA honeycomb cordierite ceramic monolith catalyst is displayed in Table 3. The substrate is a porous media with the porosity of 0.4. The powder Cu-CHA catalyst is washcoated on the walls of small channels.

Table 3. Structural physical parameters of Cu-CHA honeycomb cordierite ceramic catalyst.

Parameter	Value/Unit
Cross sectional area of channel	1 mm^2
Wall thickness of substrate	150 μm
Length	20 mm
Radius	20 mm
Volume	6.28 cm^3
Porosity	0.4
Washcoat weight	1.08 g
Cu content (related to washcoat)	3.9%

A three-dimension model was used to study the performance of Cu-CHA catalysts in NH_3-SCR. The model involved fluid flow in honeycomb pores, diffusion of gases, chemical reaction and heat transfer. In general, the standard SCR reaction occurring above 200 °C conforms to Eley-Rideal mechanism. Thus, Eley-Rideal mechanism model is utilized to simulate the SCR reactions of NO over Cu-CHA. Some assumptions are made in order to simplify the calculation and model.

- The inlet velocity and concentration of mixture, as well as inlet temperature, etc. uniformly distribute;
- The reactions in each channel of the Cu-CHA monolithic catalytic reactor are exactly the same;
- The mass transfer conforms to Fick's law.

The feed gases flowing in every small channel of the monolith catalyst can be divided into two parts, mainstream flow in central areas and seepage in porous areas near wall. The Naiver-Stokes (N-S) equation is used to describe the mainstream flow and the Brinkman equation is used in porous areas in the meantime:

$$\rho(\boldsymbol{u}\cdot\nabla)\boldsymbol{u} = \nabla\cdot(-p\boldsymbol{I} + \mu(\nabla\boldsymbol{u} + (\nabla\boldsymbol{u})^T)) \tag{7}$$

$$\frac{1}{\varepsilon_p}\rho(\boldsymbol{u}\cdot\nabla)\boldsymbol{u}\frac{1}{\varepsilon_p} = \nabla\cdot(-p\boldsymbol{I} + \mu\frac{1}{\varepsilon_p}(\nabla\boldsymbol{u} + (\nabla\boldsymbol{u})^T) - \frac{2}{3}\mu\frac{1}{\varepsilon_p}(\nabla\cdot\boldsymbol{u})\boldsymbol{I}) - \mu\kappa^{-1}\boldsymbol{u} \tag{8}$$

Here, ρ is fluid density, kg/m^3, $\boldsymbol{u}$ is velocity of fluid, m/s, p is pressure, Pa, μ is dynamic viscosity, N·s/m^2, ε_p is porosity of porous area near wall, $\boldsymbol{I}$ is unit tensor and κ is permeability.

Then, mass transfer equation is written as:

$$\nabla\cdot(-D_{F,j}\nabla C_i) + \boldsymbol{u}\cdot\nabla C_i = R_i \tag{9}$$

$$D_{F,j} = f(\Omega_D, \sigma, \varepsilon/k_b) \tag{10}$$

$$\Omega_D = f(\mu_D, \sigma, k_b, T) \tag{11}$$

In the equation above, D_{Fj} is the diffusion coefficient of the reaction gases, m^2/s, C_i is the concentration of reactant i, mol/m^3, R_i is the rate of chemical reaction. $D_{F,j}$ is a value related to the collision integral Ω_D, the characteristic length of the potential σ (m), the minimum potential energy ε/k_b (K) and dipole moment μ_D (D). These parameters can be got directly in the CHEMKIN.

Heat transfer, chemical reactions and thermal boundary conditions can change the internal temperature of the catalyst. So, the energy equation is given by:

$$\rho c_{P,L}\boldsymbol{u}\cdot\nabla T = \nabla\cdot(k\nabla T) + Q \tag{12}$$

In this equation, $C_{P,L}$ is heat capacity of gases, J/(kg·K), k is thermal conductivity, W/(m·K), Q is heat source, W/m^3.

Some boundary conditions are set as follow. The temperature for inlet feed mixture is in the range of 150–375 °C and ambient temperature is 50 °C. The mixture gases get into the reactor at a flow rate of 3000 mL/min with C_{NH3} = C_{NO} = 750 ppm, C_{O2} = 6%, C_{H2O} = 5% and C_{NO2} = C_{N2} =0 ppm. The outlet pressure is 1 atm. Also, convective heat transfer around the side and the outlet walls in the model are considered and the convective heat transfer coefficients h are 25 W/(m^2·K) and 10 W/(m^2·K) respectively.

It is well known that water can affect the catalytic efficiency of catalysts. As mentioned above, some experimental researches have proved that H_2O has an advantage in NO conversion of NH_3-SCR on Cu-CHA catalyst. In order to investigate the influence of H_2O on the NO conversion, two kinds of global kinetic models are built. The model without H_2O in feed gases comes from De-La-Torre, et al. [25], and the model with H_2O originates from Metkar, et al. [26]. Both models use one single site and apply Arrhenius to define the rate equations. Tables 4 and 5 show the reactions with related parameters of two models respectively.

Here, in Tables 4 and 5, A_{if} is the forward pre-exponential factor and A_{ib} is the backward pre-exponential factor, E_{if} is the forward activation energy and E_{ib} is the backward activation energy. In Table 4, $A_{2b} = A_{2f}/(8.61 \times 10^{-4}$ m$^{1.5}$·mol$^{-0.5})$, E_{2b} = 57.28 kJ/mol. C_i means the concentration of reactant i. Besides, K_{NH3} is equilibrium constant of NH_3 adsorption and desorption while θ_{NH3} is the adsorption rate of NH_3. In Table 5, K^* is the suppressing co-efficiency of NH_3 adsorption, which is equal to zero in Cu-CHA catalyst.

Table 4. Kinetic model without H_2O in feed gases [25].

Reactions	Rate Equations	A_{if}	E_{if}
$4NH_3 + 3O_2 \rightarrow 2N_2 + 6H_2O$	$R_1 = A_{1f}e^{(-E_1/(RT))}C_{NH_3}C_{O_2}/(1 + C_{NH_3}K_{NH_3})$	1.59×10^{12} $m^6/(g{\cdot}h{\cdot}mol)$	108.11 kJ/mol
$2NO + O_2 \leftrightarrow 2NO_2$	$R_2 = A_{2f}e^{(-E_{2f}/(RT))}C_{NO}C_{O_2}^{0.5} - A_{2b}e^{(-E_{2b}/(RT))}C_{NO_2}$	6.81×10^5 $mol/(m^3{\cdot}s)$	12.39 kJ/mol
$4NH_3 + 4NO + O_2 \rightarrow 4N_2 + 6H_2O$	$R_3 = A_{3f}e^{(-E_{3f}/(RT))}C_{NH_3}C_{NO}C_{O_2}/(1 + C_{NH_3}K_{NH_3})$	1.09×10^{12} $m^9/(g{\cdot}h{\cdot}mol^2)$	91.45 kJ/mol
$2NH_3 + NO + NO_2 \rightarrow 2N_2 + 3H_2O$	$R_4 = A_{4f}e^{(-E_{4f}/(RT))}C_{NH_3}C_{NO}C_{NO_2}/(1 + C_{NH_3}K_{NH_3})$	9.40×10^9 $m^9/(g{\cdot}h{\cdot}mol^2)$	41.98 kJ/mol
$8NH_3 + 6NO_2 \rightarrow 7N_2 + 12H_2O$	$R_5 = A_{5f}e^{(-E_{5f}/(RT))}C_{NH_3}C_{NO_2}/(1 + C_{NH_3}K_{NH_3})$	3.07×10^{12} $m^6/(g{\cdot}h{\cdot}mol)$	118.10 kJ/mol
$6NH_3 + 8NO_2 \rightarrow 7N_2O + 9H_2O$	$R_6 = A_{6f}e^{(-E_{6f}/(RT))}C_{NH_3}C_{NO_2}/(1 + C_{NH_3}K_{NH_3})$	4.48×10^{18} $m^6/(g{\cdot}h{\cdot}mol)$	152.34 kJ/mol
$2N_2O \rightarrow 2N_2 + O_2$	$R_7 = A_{7f}e^{(-E_{7f}/(RT))}C_{N_2O}C_{NO_2}$	2.45×10^{28} $m^6/(g{\cdot}h{\cdot}mol)$	257.92 kJ/mol
K_{NH_3}	$K_{NH_3} = A_{NH_3}e^{(-E_{NH_3}/(RT))}$	7.66×10^{-7} m^3/mol	−99.19 kJ/mol

Table 5. Kinetic model with H_2O in feed gases [26].

Reactions	Rate Equations	A_{if}	E_{if}
$4NH_3 + 3O_2 \rightarrow 2N_2 + 6H_2O$	$R_1 = A_{1f}e^{(-E_1/(RT))}C_{O_2}\theta_{NH_3}$	5.56×10^{16} $mol/(m^3{\cdot}s)$	178.8 kJ/mol
$2NO + O_2 \leftrightarrow 2NO_2$	$R_2 = A_{2f}e^{(-E_{2f}/(RT))}C_{NO}C_{O_2}^{0.5} - A_{2b}e^{(-E_{2b}/(RT))}C_{NO_2}$	5.10×10^7 $mol/(m^3{\cdot}s)$	56.0 kJ/mol
$4NH_3 + 4NO + O_2 \rightarrow 4N_2 + 6H_2O$	$R_3 = A_{3f}e^{(-E_{3f}/(RT))}C_{NO}/(1 + C_{NH_3}K^*)$	7.08×10^{13} $mol/(m^3{\cdot}s)$	89.1 kJ/mol
$2NH_3 + NO + NO_2 \rightarrow 2N_2 + 3H_2O$	$R_4 = A_{4f}e^{(-E_{4f}/(RT))}C_{NO}C_{NO_2}\theta_{NH_3}$	1.00×10^{18} $mol/(m^3{\cdot}s)$	77.1 kJ/mol
$8NH_3 + 6NO_2 \rightarrow 7N_2 + 12H_2O$	$R_5 = A_{5f}e^{(-E_{5f}/(RT))}C_{NO_2}\theta_{NH_3}$	1.96×10^{17} $mol/(m^3{\cdot}s)$	136.3 kJ/mol
$2NH_3 + 2NO_2 \rightarrow N_2 + NH_4NO_3 + H_2O$	$R_6 = A_{6f}e^{(-E_{6f}/(RT))}C_{NO_2}\theta_{NH_3}$	2.28×10^8 $mol/(m^3{\cdot}s)$	43.0 kJ/mol
$NH_4NO_3 \rightarrow N_2O + 2H_2O$	$R_7 = A_{7f}e^{(-E_{7f}/(RT))}C_{NH_4NO_3}$	1.25×10^8 $mol/(m^3{\cdot}s)$	41.5 kJ/mol

4. Grid Independence and Validation Test of Method

4.1. Grid Independence Verification

Generally speaking, the denser the mesh is, the smaller the error generated in the calculation. However, the mesh cannot be infinitely refined due to the finite computational ability. To ensure the accuracy of the calculation results, it is necessary to find a suitable grid, which can reduce the calculation error and speed up the calculation. In our study, several different grids with number of 5346, 11,040, 22,260, 24,225, 29,070, 32,300, 44,980 are used to verify the independence of grid density, with the inlet temperature T = 150 °C and being without H_2O in feed gases. Table 6 shows the results of grid independence test, which presents the variation of C_{NO} and C_{NH3} at outlet and NO conversion, respectively.

Table 6. The variation results of calculation with grid number.

Grid Number	Outlet C_{NO}	Relative Variation	NO Conversion	Relative Variation	Outlet C_{NH3}	Relative Variation
5346	5.860×10^{-4}	/	0.21867	/	6.958×10^{-4}	/
11,040	6.151×10^{-4}	4.7340%	0.17984	17.7561%	7.053×10^{-4}	1.3413%
22,260	6.217×10^{-4}	1.0600%	0.17105	4.8858%	7.074×10^{-4}	0.3025%
29,070	6.291×10^{-4}	0.0318%	0.16119	0.1654%	7.099×10^{-4}	0.0099%
32,300	6.290×10^{-4}	0.0127%	0.16129	0.0661%	7.099×10^{-4}	0.0028%
44,980	6.289×10^{-4}	0.0014%	0.16141	0.0743%	7.098×10^{-4}	0.0183%

It can be seen from the Table 6, with the increase of grid number, the relative variations of C_{NO}, C_{NH3} and NO conversion become smaller. Actually, if comparing the variation between the Grid 5 (32,300) and 6 (44,980), it can be found that although the number of grid is increased by nearly 40%, the relative variations of outlet C_{NO}, C_{NH3} and NO conversion is small, being 0.001%, 0.018% and 0.074% respectively. Therefore, Grid 5 (32,300) is used in this investigation to ensure balances between the accuracy and the grid density.

4.2. Validation against Experimental Results

In order to demonstrate the accuracy of the present developed model, two sets of experimental data are selected as the verification benchmarks. These experimental data are acquired from De-La-Torre's work [23], because the boundary conditions, the structure and physicochemical properties of catalyst they used for SCR and other operating conditions are the most similar to ours. More details of the reactor's dimension and operating condition refer to the reference [23].

Tables 7 and 8 list relative errors of NO and NH_3 conversion between experimental and simulated results under different operating conditions to show the validation of the numerical model.

Table 7. The results with relative errors of NO conversion between experiment and simulation under two operating conditions.

Temperature (°C)	NO Conversion (Without H_2O)			NO Conversion (With 5% H_2O)		
	Experiment	Simulation	Relative Error	Experiment	Simulation	Relative Error
150	15.000%	16.092%	7.280%	16.500%	18.055%	9.424%
200	66.200%	72.744%	9.885%	66.700%	72.813%	9.165%
250	98.000%	99.057%	1.079%	99.300%	98.580%	0.725%
300	90.100%	84.164%	6.588%	91.700%	95.101%	3.709%
350	45.060%	50.912%	12.987%	68.920%	77.745%	12.805%
375	21.200%	26.717%	26.024%	38.000%	54.664%	30.484%
average	/		10.641%	/		11.052%

Table 8. The results with relative errors of NH_3 conversion between experiment and simulation under two operating conditions.

Temperature (°C)	Without H_2O			With 5% H_2O		
	Experiment	Simulation	Relative Error	Experiment	Simulation	Relative Error
150	13.200%	15.336%	16.182%	16.830%	17.852%	6.072%
200	44.340%	42.516%	4.114%	55.460%	72.113%	30.027%
250	78.030%	74.300%	4.780%	80.820%	98.289%	21.615%
300	98.210%	96.317%	1.928%	98.600%	100.000%	1.420%
350	100.000%	99.999%	0.001%	100.000%	100.000%	0.000%
375	100.000%	100.000%	0.000%	100.000%	100.000%	0.000%
average	/		4.501%	/		9.856%

From these tables, it is apparent that a very good agreement has been obtained, the average errors of NO conversion are only 10.641% (without H_2O) and 11.052% (with H_2O) between the experimental data and simulated outcomes. Simultaneously, the average errors of NH_3 conversion are 4.501% (without H_2O) and 9.856% (with H_2O) respectively. The average errors with 5% H_2O are a little higher than that without H_2O. The maximum deviations is 30.484% (at T = 375 °C with 5% H_2O, in NO conversion), while the minimum is close to 0% (at T = 350 °C and 375 °C for with and without H_2O, in NH_3 conversion). The results obtained, thus far, have clearly indicated that the catalytic reactor model presented in this study predicts well the catalyst's global performance, and it can readily be employed for further simulation studies.

5. Conclusions

A three dimensionally numerical model including global kinetic chemical reactions, fluid dynamics, heat and mass transfer was built for a Cu-CHA catalyst reactor by COMSOL Multiphysics with 32,300 grid numbers. And several structural and operating conditions of NH_3-SCR system were researched respectively to investigate the influence on the performance of Cu-CHA catalyst.

The presence of H_2O in feed gases can increase the denitrification efficiency of Cu-CHA catalyst at medium temperature range (250–375 °C) and improves the NH_3 conversion especially at low temperature range (150–250 °C). It inhibits NH_3 oxidation, increases Cu reducibility and Bronsted acidity, causing higher NO conversion for Cu-CHA than that without water.

The C_{O2} has almost no influence on catalytic performance of Cu-CHA catalyst, possibly because the existence of NO and NO_2 in reactant have higher oxidation ability than O_2 and concentration of reactants is low. By ascending the ratio of NO_2 to NO_x, the outlet C_{NO} declines, C_{N2} firstly increases and then decreases and C_{N2O} continues to rise. The balanced point is x_0 = 0.5, where fast SCR prevails and Cu-CHA catalyst performs high NO conversion and yield of N_2, extremely low output of N_2O as well. With the ratio of NH_3 to NO_x (ANR) increase, outlet C_{NO} gradually declines while C_{NH3} rapidly grows when ANR > 1. The appropriate value of ANR is approximately 1.1, where Cu-CHA catalyst has great denitrification efficiency and low NH_3 escape.

Increasing inlet flow velocity leads to worse denitrification performance of Cu-CHA catalyst, which may be due to insufficient react time between feed gases and catalyst. As the length of channels increases by 20 mm, the denitrification efficiency is enhanced by about 10% evenly, owing to providing more contact areas. In addition, the change of cross area of channels and wall thickness have great influence on NO conversion by affecting WHSV in reaction system. Bigger cross area causes larger WHSV, resulting in lower NO abatement efficiency. In contrast, thicker wall of channels brings lower WHSV, leading to longer residence time of exhaust gases and higher NO conversion of the reactor. However, the effect of WHSV is finite which may because the total mass of Cu-CHA catalyst is fixed.

Author Contributions: Validation, writing—review & editing, Y.L.; Conceptualization, methodology, software, formal analysis, investigation, resources, data curation, visualization, writing—original draft, Y.Z. and N.Z.; Project administration, funding acquisition Y.L. and Z.L. All authors have read and agreed to the published version of the manuscript.

Funding: This research was funded by Beijing Natural Science Foundation (3192008) and the National Key R&D Program of China (No. 2017YFB0504000).

Data Availability Statement: The data presented in Table 4 are available in http://dx.doi.org/10.1016/j.cattod.2017.04.011 (accessed on 26 June 2021). The data presented in Table 5 are available in http://dx.doi.org/10.1016/j.ces.2012.09.008 (accessed on 26 June 2021). The data presented in Figure 1 (experiment) and Figure 2 (experiment) are available in http://dx.doi.org/10.1016/j.apcatb.2016.01.020 (accessed on 26 June 2021).

Acknowledgments: We acknowledge editors and reviewers' generous help and guidance.

Conflicts of Interest: The authors declare no conflict of interest.

References

1. Shan, Y.; Shi, X.; He, G.; Liu, K.; Yan, Z.; Yu, Y.; He, H. Effects of NO_2 Addition on the NH_3-SCR over Small-Pore Cu–SSZ-13 Zeolites with Varying Cu Loadings. *J. Phys. Chem. C* **2018**, *122*, 25948–25953. [CrossRef]
2. Zhu, N.; Shan, Y.; Shan, W.; Sun, Y.; Liu, K.; Zhang, Y.; He, H. Distinct NO_2 Effects on Cu-SSZ-13 and Cu-SSZ-39 in the Selective Catalytic Reduction of NO_x with NH_3. *Environ. Sci. Technol.* **2020**, *54*, 15499–15506. [CrossRef]
3. Sierraalta, A.; Añez, R.; Brussin, M.-R. Theoretical Study of the Interaction of NO_2 Molecule with a Metal−Zeolite Model (Metal = Cu, Ag, Au). *J. Phys. Chem. A* **2002**, *106*, 6851–6856. [CrossRef]
4. Kamasamudram, K.; Currier, N.W.; Chen, X.; Yezerets, A. Overview of the practically important behaviors of zeolite-based urea-SCR catalysts, using compact experimental protocol. *Catal. Today* **2010**, *151*, 212–222. [CrossRef]
5. Deng, D.; Deng, S.; He, D.; Wang, Z.; Chen, Z.; Ji, Y.; Yan, G.; Hou, G.; Liu, L.; He, H. A comparative study of the hydrothermal aging effect on cerium and lanthanum doped Cu/SSZ-13 catalysts for NH_3-SCR. *J. Rare Earths* **2020**, *39*, 969–978. [CrossRef]
6. Zhang, J.; Shan, Y.; Zhang, L.; Du, J.; He, H.; Han, S.; Lei, C.; Wang, S.; Fan, W.; Feng, Z.; et al. Importance of controllable Al sites in CHA framework by crystallization pathways for NH_3-SCR reaction. *Appl. Catal. B Environ.* **2020**, *277*, 119193. [CrossRef]
7. Leistner, K.; Mihai, O.; Wijayanti, K.; Kumar, A.; Kamasamudram, K.; Currier, N.W.; Yezerets, A.; Olsson, L. Comparison of Cu/BEA, Cu/SSZ-13 and Cu/SAPO-34 for ammonia-SCR reactions. *Catal. Today* **2015**, *258*, 49–55. [CrossRef]
8. Nova, I.; Tronconi, E. Kinetic study of the NO/NO_2-NH_3 SCR reactions over a V_2O_5–WO_3/TiO_2 commercial catalyst for the after treatment of Diesel engines exhausts. *IFAC Proc. Vol.* **2009**, *42*, 183–190. [CrossRef]
9. Usberti, N.; Jablonska, M.; Blasi, M.D.; Forzatti, P.; Lietti, L.; Beretta, A. Design of a "high-efficiency" NH_3-SCR reactor for stationary applications. A kinetic study of NH_3 oxidation and NH_3-SCR over V-based catalysts. *Appl. Catal. B Environ.* **2015**, *179*, 185–195. [CrossRef]
10. Gao, F.; Wang, Y.; Kollár, M.; Washton, N.M.; Szanyi, J.; Peden, C.H.F. A comparative kinetics study between Cu/SSZ-13 and Fe/SSZ-13 SCR catalysts. *Catal. Today* **2015**, *258*, 347–358. [CrossRef]
11. Olsson, L.; Wijayanti, K.; Leistner, K.; Kumar, A.; Joshi, S.Y.; Kamasamudram, K.; Currier, N.W.; Yezerets, A. A multi-site kinetic model for NH_3-SCR over Cu/SSZ-13. *Appl. Catal. B Environ.* **2015**, *174–175*, 212–224. [CrossRef]
12. Usberti, N.; Gramigni, F.; Nasello, N.D.; Iacobone, U.; Selleri, T.; Hu, W.; Liu, S.; Gao, X.; Nova, I.; Tronconi, E. An experimental and modelling study of the reactivity of adsorbed NH_3 in the low temperature NH_3-SCR reduction half-cycle over a Cu-CHA catalyst. *Appl. Catal. B Environ.* **2020**, *279*, 119397. [CrossRef]
13. Eijima, W.; Shibata, G.; Shibayama, N.; Kobashi, Y.; Ogawa, H.; Shimizu, K.-I. Kinetic modeling of steady-state NH_3-SCR over a monolithic Cu-CHA catalyst. *Catal. Today* **2020**, *352*, 237–242. [CrossRef]
14. Joshi, S.Y.; Kumar, A.; Luo, J.; Kamasamudram, K.; Currier, N.W.; Yezerets, A. Combined experimental and kinetic modeling study of the bi-modal NO conversion profile on commercial Cu-SAPO-34 catalyst under standard SCR conditions. *Appl. Catal. B Environ.* **2015**, *165*, 27–35. [CrossRef]
15. Wang, D.; Jangjou, Y.; Liu, Y.; Sharma, M.K.; Luo, J.; Li, J.; Kamasamudram, K.; Epling, W.S. A comparison of hydrothermal aging effects on NH_3-SCR of NOx over Cu-SSZ-13 and Cu-SAPO-34 catalysts. *Appl. Catal. B Environ.* **2015**, *165*, 438–445. [CrossRef]
16. Yu, T.; Wang, J.; Shen, M.; Wang, J.; Li, W. The influence of CO_2 and H_2O on selective catalytic reduction of NO by NH_3 over Cu/SAPO-34 catalyst. *Chem. Eng. J.* **2015**, *264*, 845–855. [CrossRef]
17. Wang, L.; Gaudet, J.R.; Li, W.; Weng, D. Migration of Cu species in Cu/SAPO-34 during hydrothermal aging. *J. Catal.* **2013**, *306*, 68–77. [CrossRef]
18. Fahami, A.R.; Nova, I.; Tronconi, E. A kinetic modeling study of NO oxidation over a commercial Cu-CHA SCR catalyst for diesel exhaust aftertreatment. *Catal. Today* **2017**, *297*, 10–16. [CrossRef]
19. Gao, Z.; Pihl, J.; LaClair, T.; Fricke, B. Global kinetic modeling of NH_3-SCR with two sites of NH_3 storage on Cu-SSZ-13. *Chem. Eng. J.* **2021**, *406*, 127120. [CrossRef]

20. Guo, K.; Ji, J.; Osuga, R.; Zhu, Y.; Sun, J.; Tang, C.; Kondo, J.N.; Dong, L. Construction of Fe_2O_3 loaded and mesopore confined thin-layer titania catalyst for efficient NH_3-SCR of NO_x with enhanced H_2O/SO_2 tolerance. *Appl. Catal. B Environ.* **2021**, *287*, 119982. [CrossRef]
21. Lei, Z.; Han, B.; Yang, K.; Chen, B. Influence of H_2O on the low-temperature NH_3-SCR of NO over V_2O_5/AC catalyst: An experimental and modeling study. *Chem. Eng. J.* **2013**, *215–216*, 651–657. [CrossRef]
22. Zhang, N.; He, H.; Wang, D.; Li, Y. Challenges and opportunities for manganese oxides in low-temperature selective catalytic reduction of NO_x with NH_3: H_2O resistance ability. *J. Solid State Chem.* **2020**, *289*, 121464. [CrossRef]
23. De-La-Torre, U.; Pereda-Ayo, B.; Moliner, M.; González-Velasco, J.R.; Corma, A. Cu-zeolite catalysts for NOx removal by selective catalytic reduction with NH_3 and coupled to NO storage/reduction monolith in diesel engine exhaust aftertreatment systems. *Appl. Catal. B Environ.* **2016**, *187*, 419–427. [CrossRef]
24. Shin, Y.; Jung, Y.; Cho, C.P.; Pyo, Y.D.; Jang, J.; Kim, G.; Kim, T.M. NOx abatement and N_2O formation over urea-SCR systems with zeolite supported Fe and Cu catalysts in a nonroad diesel engine. *Chem. Eng. J.* **2020**, *381*. [CrossRef]
25. De-La-Torre, U.; Pereda-Ayo, B.; Gutiérrez-Ortiz, M.A.; González-Marcos, J.A.; González-Velasco, J.R. Steady-state NH_3-SCR global model and kinetic parameter estimation for NO_x removal in diesel engine exhaust aftertreatment with Cu/chabazite. *Catal. Today* **2017**, *296*, 95–104. [CrossRef]
26. Metkar, P.S.; Harold, M.P.; Balakotaiah, V. Experimental and kinetic modeling study of NH_3-SCR of NO_x on Fe-ZSM-5, Cu-chabazite and combined Fe- and Cu-zeolite monolithic catalysts. *Chem. Eng. Sci.* **2013**, *87*, 51–66. [CrossRef]